












RESEARCH PAPER



Tetrahydroquinazole-based secondary sulphonamides as carbonic anhydrase inhibitors: synthesis, biological evaluation against isoforms I, II, IV, and IX, and computational studies

Emma Baglini^a , Rahul Ravichandran^b , Emanuela Berrino^c , Silvia Salerno^a , Elisabetta Barresi^a , Anna Maria Marini^a , Monica Viviano^d , Sabrina Castellano^d, Federico Da Settimo^a , Claudiu T. Supuran^c , Sandro Cosconati^b  and Sabrina Taliani^a 

^aDepartment of Pharmacy, University of Pisa, Pisa, Italy; ^bDiSTABIF, University of Campania Luigi Vanvitelli, Caserta, Italy; ^cNEUROFARBA Department, Sezione di Scienze Farmaceutiche e Nutraceutiche, Università degli Studi di Firenze, Sesto Fiorentino, Italy; ^dDepartment of Pharmacy, Epigenetic Med Chem Lab, University of Salerno, Fisciano, Italy

ABSTRACT

A library of variously decorated *N*-phenyl secondary sulphonamides featuring the bicyclic tetrahydroquinazole scaffold was synthesised and biologically evaluated for their inhibitory activity against human carbonic anhydrase (hCA) I, II, IV, and IX. Of note, several compounds were identified showing submicromolar potency and excellent selectivity for the tumour-related hCA IX isoform. Structure–activity relationship data attained for various substitutions were rationalised by molecular modelling studies in terms of both inhibitory activity and selectivity.

ARTICLE HISTORY

Received 9 June 2021
Revised 8 July 2021
Accepted 13 July 2021

KEYWORDS

Carbonic anhydrases inhibitors; secondary sulphonamides; tetrahydroquinazole derivatives; structure–activity relationships; tumour-related CA IX isoform

Introduction

Carbonic anhydrases (CAs) are ubiquitous zinc enzymes that catalyse the reversible hydration of carbon dioxide to bicarbonate by a metal hydroxide nucleophilic mechanism¹. CAs play key roles in several physiological processes, such as pH and CO₂ homeostasis, respiration, secretion of electrolytes in a variety of tissues/organs, biosynthetic reactions, including lipogenesis, gluconeogenesis, ureagenesis, calcification, bone resorption, and tumorigenicity^{2–5}. To date, 15 different isoforms of human CAs (hCAs) have been identified with different catalytic activities, cellular and subcellular localisation, and tissue distributions⁶: CA I, CA II, CA III, CA VII, and CA XIII isoforms are cytosolic, CA IV, CA IX, CA XII, CA XIV, and CA XV are transmembrane bound, CA VA and CA VB are mitochondrial and CA VI is secreted in saliva and milk^{7,8}. Isoforms VIII, X, and XI are cytosolic, acatalytic, and preponderantly expressed within the brain, but their functions remain elusive.

Many hCA isoenzymes are considered promising therapeutic targets in the development of potentially valuable new small molecules for the treatment or prevention of many diseases such as glaucoma, epilepsy, obesity, and cancer^{9,10}. Indeed, CA inhibitors (CAIs) have been in clinical use for many decades as diuretics and systemically acting antiglaucoma drugs; many CAIs are primary sulphonamides (acetazolamide (AAZ, Chart 1), ethoxzolamide, dichlorphenamide) coordinating the zinc ion present in the catalytic site through their deprotonated sulphonamide nitrogen

atom¹¹. However, the high sequence homology between hCA isoforms, combined with their widespread and ubiquitous tissue localisation, makes the discovery of CAIs with functional selectivity for a specific target isoform a major challenge in the development of potential drugs, free from off-target side effects¹².

In the last decades, several tricyclic/bicyclic scaffolds, decorated with a primary sulphonamide moiety, have been exploited by our research group, leading to the identification of several derivatives with high CA inhibitory activity and promising selectivity profiles^{13–15}. In particular, tricyclic primary benzenesulfonamides featuring the benzothioopyrano[4,3-*c*]pyrazole and pyridothioopyrano[4,3-*c*]pyrazole systems (see general formula I, Chart 1) were initially developed as geometrically constrained analogues of celecoxib (CLX, Chart 1) and valdecoxib (VLX, Chart 1), cyclooxygenase 2 (COX-2) specific inhibitors that act also as potent CAIs^{6,13}. Based on the encouraging results obtained and the SAR outlined, our project on CAIs was pursued, always within primary benzenesulfonamide-based small molecules, following two different approaches: (i) investigation of three different, but structurally related, tricyclic scaffolds, that is benzo/pyrido-thioopyranopyrimidine II and pyrazolodihydroquinazoline III (Chart 1)^{14,15}; (ii) structural simplification of the core scaffolds of I and II to yield bicyclic tetrahydroindazole IV and tetrahydroquinazole V derivatives, respectively, in which the phenyl- or pyrido-fused moiety was removed (Chart 1)¹⁵.

CONTACT Silvia Salerno  silvia.salerno@unipi.it  Department of Pharmacy, University of Pisa, Via Bonanno Pisano, 6, Pisa 56126, Italy; Sandro Cosconati  sandro.cosconati@unicampania.it  DiSTABIF, University of Campania Luigi Vanvitelli, Caserta, Italy

© 2021 The Author(s). Published by Informa UK Limited, trading as Taylor & Francis Group.

This is an Open Access article distributed under the terms of the Creative Commons Attribution License (<http://creativecommons.org/licenses/by/4.0/>), which permits unrestricted use, distribution, and reproduction in any medium, provided the original work is properly cited.

More recently, the tetrahydroindazole scaffold of class **IV** was further exploited by the development of a library of *N*-phenyl-secondary sulphonamides, variously decorated at para- or meta-position with groups characterised by different electron-donor/acceptor capabilities (**VI**, Chart 1)¹⁶. Indeed, although secondary and tertiary sulphonamides have been recently reported as efficient and selective inhibitors of the cancer-related hCA IX and XII isoforms,^{17–25} the chemical space of such CAls remains so far rarely explored and their binding mode is still a subject of investigation²⁶.

For what concerns class **VI**, although, in general, the insertion of a secondary sulphonamide function on the tetrahydroindazole scaffold produced inhibitors with a moderate micromolar potency, lower than the primary sulphonamide parent compounds of series **IV**, some interesting structure–activity relationship (SAR) data were acquired and rationalised through theoretical studies¹⁶. Specifically, the inhibitory profile of the novel indazolyl-*N*-arylbenzenesulfonamides **VI** appears strictly dependent on the substitution pattern at 6-position, with the 6-phenyl group able to produce hCA II inhibitors with good potency and selectivity¹⁶.

Pursuing our interest in the development of secondary sulphonamide CAls, in the present study, we turned our attention to the bicyclic tetrahydroquinazolinone scaffold of class **V**. Thus, derivatives **1–12** (Chart 1) were synthesised and biologically evaluated for their enzyme inhibitory activity against four physiologically relevant CA isoforms, the hCA I, II, IV, and IX. In the novel compounds, the secondary benzenesulfonamide moiety was decorated at *para* position with groups of various nature ($R_3=H, OCH_3, NO_2, CH_3$) to modulate the acidity of the sulphonamide itself, keeping in mind the groups conferring the best results, in terms of potency and selectivity, in series **VI**; in addition, the same substituents of the corresponding primary sulphonamides **V** described by us¹⁵ were maintained at 7-position ($R_1=R_2=H; R_1=H, R_2=C_6H_5; R_1=R_2=CH_3$).

Materials and methods

Chemistry

The uncorrected melting points were determined using a Reichert Köfler hot-stage apparatus. NMR spectra were obtained on a Bruker AVANCE 400 (¹H, 400 MHz, ¹³C, 100 MHz) in DMSO-*d*₆. Chemical shifts are expressed in δ (ppm) and coupling constants (*J*) in Hertz. Magnesium sulphate was used as the drying agent. Evaporations were made *in vacuo* (rotating evaporator). Analytical TLC have been carried out on Merck 0.2 mm pre-coated silica gel aluminium sheets (60 F-254). Silica gel 60 (230–400 mesh) was used for column chromatography. Microwave (MW) assisted reactions were carried out in BIOTAGE Initiator 2.5 microwave apparatus. The purity of the target inhibitors **1–12** was determined, using a Shimadzu LC-20AD SP liquid chromatograph equipped with a DDA Detector (Kyoto, Japan) at 220 nm (column C18 (250 mm \times 4.6 mm, 5 μ m, Shim-pack)). The mobile phase, delivered at isocratic flow, consisted of methanol (80%) and water (20%) and a flow rate of 1.0 ml/min. All the compounds showed percent purity values of >95%. Reagents, starting materials, and solvents were purchased from commercial suppliers and used as received. The following intermediates were obtained according to previously described procedures: 2-[(dimethylamino)methylene]cyclohexan-1,3-dione **14a**²⁷, 2-[(dimethylamino)methylene]-5-phenylcyclohexan-1,3-dione **14b**²⁷, 2-[(dimethylamino)methylene]-5,5-dimethylcyclohexan-1,3-dione **14c**²⁷, and *N*-(4-aminosulfonyl)phenylguanidine carbonate **15**¹⁴.

General procedure for the synthesis of 4-((5-oxo-5,6,7,8-tetrahydroquinazolin-2-yl)amino)benzenesulfonamide derivatives **16a–c**

A mixture of the proper 2-(dimethylamino)methylene-1,3-dione derivative **14a–c** (0.45 mmol), *N*-(4-aminosulfonyl)phenylguanidine carbonate **15** (0.25 g, 0.90 mmol) and NaOH (54 mg, 1.35 mmol) in 5 ml of *n*-BuOH was irradiated at a $T=160^\circ\text{C}$ (pre-stirring time = 3 min) for 40 min. After cooling, the obtained crude solid compounds **16a–c** were purified by recrystallisation from ethanol.

4-((5-oxo-5,6,7,8-tetrahydroquinazolin-2-yl)amino)benzenesulfonamide (**16a**). Yield 66%; m.p. 294–296 $^\circ\text{C}$ ¹⁵.

4-((5-oxo-7-phenyl-5,6,7,8-tetrahydroquinazolin-2-yl)amino)benzenesulfonamide (**16b**). Yield 70%; m.p. 214–215 $^\circ\text{C}$ ¹⁵.

4-((5-oxo-7,7-dimethyl-5,6,7,8-tetrahydroquinazolin-2-yl)amino)benzenesulfonamide (**16c**). Yield 72%; m.p. 258–260 $^\circ\text{C}$ ¹⁵.

General procedure for the synthesis of *N*-aryl-4-((5-oxo-5,6,7,8-tetrahydroquinazolin-2-yl)amino)benzenesulfonamide derivatives **1–12**

To a solution of the proper 4-(5-oxo-7-substituted-5,6,7,8-tetrahydroquinazolin-2-yl)amino)benzenesulfonamide **16a–c** (0.94 mmol) in dry MeCN (10 ml) at room temperature, CuI (8 mg, 0.04 mmol), anhydrous K₂CO₃ (0.28 g, 2.07 mmol), the proper aryl iodide (1.13 mmol), and DMEDA (0.04 ml, 0.38 mmol) were added, and the resulting mixture was heated at 100 $^\circ\text{C}$ for 8–24 h (TLC analysis). After cooling, the reaction mixture was diluted with water (20 ml), acidified with 2.0 N HCl to pH = 4, and extracted with EtOAc (3 \times 20 ml). The organic phase was dried (MgSO₄), filtered and evaporated under reduced pressure. The crude material was purified by flash chromatography using PE/EtOAc as eluting system, to afford compounds **1–12**.

4-((5-Oxo-5,6,7,8-tetrahydroquinazolin-2-yl)amino)-*N*-phenylbenzenesulfonamide (**1**)

Compound **1** was obtained as a solid (0.093 g, 25%) starting from compound **16a** (0.30 g) and iodobenzene (0.13 ml); m.p. 281–283 $^\circ\text{C}$; ¹H NMR (400 MHz, DMSO-*d*₆): δ 2.04–2.07 (m, 2H), 2.57 (t, *J* = 6.4 Hz, 2H), 2.93 (t, *J* = 6.0 Hz, 2H), 6.99 (t, *J* = 7.2 Hz, 1H), 7.09 (d, *J* = 7.6 Hz, 2H), 7.19–7.23 (m, 2H), 7.70 (d, *J* = 8.8 Hz, 2H), 7.94 (d, *J* = 8.8 Hz, 2H), 8.84 (s, 1H), 10.19 (s, 1H), 10.67 (s, 1H). ¹³C NMR (100 MHz, DMSO-*d*₆): δ 21.0, 31.8, 38.0, 119.3 (2C), 119.5 (2C), 120.2, 124.4, 128.2 (2C), 129.6 (2C), 132.7, 138.1, 143.8, 158.2, 160.4, 174.2, 195.8.

N-(4-methoxyphenyl)-4-((5-oxo-5,6,7,8-tetrahydroquinazolin-2-yl)amino)benzenesulfonamide (**2**)

Compound **2** was obtained as a solid (0.080 g, 20%) starting from compound **16a** (0.30 g) and 1-iodo-4-methoxybenzene (0.26 g); m.p. 233–235 $^\circ\text{C}$. ¹H NMR (400 MHz, DMSO-*d*₆): δ 2.05–2.08 (m, 2H), 2.58 (t, *J* = 6.2 Hz, 2H), 2.94 (t, *J* = 6.2 Hz, 2H), 3.66 (s, 3H), 6.79 (d, *J* = 9.2 Hz, 2H), 6.98 (d, *J* = 9.2 Hz, 2H), 7.62 (d, *J* = 8.8 Hz, 2H), 7.93 (d, *J* = 9.2 Hz, 2H), 8.85 (s, 1H), 9.81 (s, 1H), 10.67 (s, 1H). ¹³C NMR (100 MHz, DMSO-*d*₆): δ 20.8, 31.6, 37.8, 55.3, 114.4 (2C), 115.1, 119.0, 119.1 (2C), 123.3 (2C), 126.1, 127.9 (2C), 130.5, 132.6, 143.4, 156.5, 157.8, 160.5, 195.3.

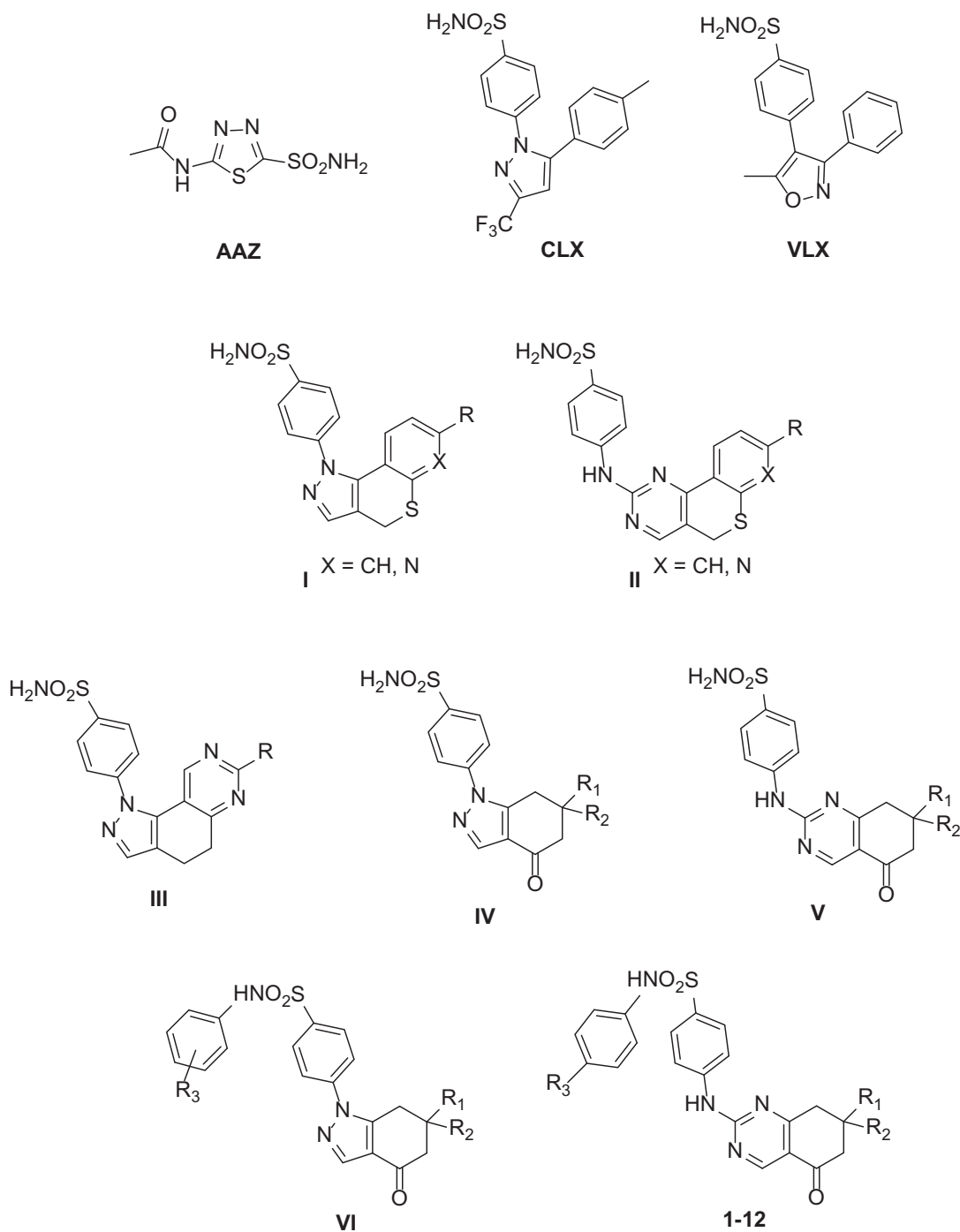


Chart 1. Structures of celecoxib (CLX), valdecoxib (VLX), acetazolamide (AAZ); structures of previously described (I–VI) and newly synthesized (1–12) CAls.]

***N*-(4-nitrophenyl)-4-((5-oxo-5,6,7,8-tetrahydroquinazolin-2-yl)amino)benzenesulfonamide (3)**

Compound **3** was obtained as a solid (0.10 g, 25%) starting from compound **16a** (0.30 g) and 1-iodo-4-nitrobenzene (0.28 g); m.p. 264–266 °C. ¹H NMR (400 MHz, DMSO-*d*₆): δ 2.05–2.08 (m, 2H), 2.58 (t, *J* = 6.4 Hz, 2H), 2.93 (t, *J* = 6.2 Hz, 2H), 7.30 (d, *J* = 9.2 Hz, 2H), 7.83 (d, *J* = 8.8 Hz, 2H), 7.99–8.02 (m, 2H), 8.13 (d, *J* = 9.2 Hz, 2H), 8.85 (s, 1H), 10.74 (s, 1H), 11.20 (s, 1H). ¹³C NMR (100 MHz, DMSO-*d*₆): δ 21.0, 31.8, 38.0, 118.2 (2C), 119.4, 119.7 (2C), 125.8 (2C), 128.4 (2C), 131.9, 142.8, 144.4, 144.7, 158.1, 160.4, 174.2, 180.3, 195.9.

4-((5-Oxo-5,6,7,8-tetrahydroquinazolin-2-yl)amino)-*N*-(4-tolyl)benzenesulfonamide (4)

Compound **4** was obtained as a solid (0.077 g, 20%) starting from compound **16a** (0.30 g) and 1-iodo-4-methylbenzene (0.25 g); m.p. 272–274 °C. ¹H NMR (400 MHz, DMSO-*d*₆): δ 2.05–2.08 (m, 2H), 2.17 (s, 3H), 2.58 (t, *J* = 6.8 Hz, 2H), 2.93 (t, *J* = 6.0 Hz, 2H), 6.96–7.03 (m, 4H), 7.66 (d, *J* = 9.2 Hz, 2H), 7.93 (d, *J* = 9.2 Hz, 2H), 8.85 (s, 1H), 10.01 (s, 1H), 10.67 (s, 1H). ¹³C NMR (100 MHz, DMSO-*d*₆): δ 20.6, 21.0, 31.8, 38.0, 119.2, 119.5 (2C), 120.8 (2C), 128.1 (2C), 129.9 (2C), 132.8, 133.7, 135.4, 143.6, 158.1, 160.4, 174.2, 195.9.

4-((5-Oxo-7-phenyl-5,6,7,8-tetrahydroquinazolin-2-yl)amino)-N-phenylbenzenesulfonamide (5)

Compound **5** was obtained as a solid (0.13 g, 30%) starting from compound **16b** (0.37 g) and iodobenzene (0.23 ml); m.p. 111–113 °C. ¹H NMR (400 MHz, DMSO-d₆): δ 2.69–2.73 (m, 2H), 2.97–3.10 (m, 2H), 3.52–3.59 (m, 1H), 6.99 (t, *J* = 7.2 Hz, 1H), 7.09 (d, *J* = 8.0 Hz, 2H), 7.19–7.28 (m, 3H), 7.34–7.40 (m, 4H), 7.69 (d, *J* = 8.8 Hz, 2H), 7.96 (d, *J* = 8.8 Hz, 2H), 8.90 (s, 1H), 10.19 (s, 1H), 10.75 (s, 1H). ¹³C NMR (100 MHz, DMSO-d₆): δ 38.3, 44.8, 118.6, 119.3, 119.9 (2C), 124.0, 127.0, 127.1 (2C), 127.9, 128.8 (2C), 129.3 (2C), 132.6, 138.0, 143.3, 143.5, 157.8, 160.5, 172.9, 194.7.

N-(4-methoxyphenyl)-4-((5-oxo-7-phenyl-5,6,7,8-tetrahydroquinazolin-2-yl)amino)benzenesulfonamide (6)

Compound **6** was obtained as a solid (0.094 g, 20%) starting from compound **16b** (0.37 g) and 1-iodo-4-methoxybenzene (0.26 g); m.p. 103–105 °C. ¹H NMR (400 MHz, DMSO-d₆): δ 2.67–2.73 (m, 2H), 2.97–3.01 (m, 2H), 3.53–3.57 (m, 1H), 3.65 (s, 3H), 6.79 (d, *J* = 9.2 Hz, 2H), 6.97 (d, *J* = 9.2 Hz, 2H), 7.26–7.28 (m, 1H), 7.34–7.40 (m, 4H), 7.61 (d, *J* = 8.8 Hz, 2H), 7.95 (d, *J* = 8.8 Hz, 2H), 8.91 (s, 1H), 9.82 (s, 1H), 10.75 (s, 1H). ¹³C NMR (100 MHz, DMSO-d₆): δ 38.4, 44.8, 55.2, 114.3 (2C), 116.8, 118.4, 119.1, 123.2 (2C), 127.0, 127.8 (2C), 128.7, 130.6 (2C), 132.6, 143.2, 156.4, 158.0, 160.5, 194.5.

N-(4-nitrophenyl)-4-((5-oxo-7-phenyl-5,6,7,8-tetrahydroquinazolin-2-yl)amino)benzenesulfonamide (7)

Compound **7** was obtained as a solid (0.14 g, 30%) starting from compound **16b** (0.37 g) and 1-iodo-4-nitrobenzene (0.28 g); m.p. 118–120 °C. ¹H NMR (400 MHz, DMSO-d₆): δ 2.67–2.73 (m, 2H), 2.97–3.04 (m, 2H), 3.54–3.56 (m, 1H), 7.26–7.30 (m, 2H), 7.34–7.40 (m, 3H), 7.82 (d, *J* = 8.8 Hz, 2H), 7.96–8.07 (m, 4H), 8.12 (d, *J* = 9.2 Hz, 2H), 8.91 (s, 1H), 10.82 (s, 1H), 11.21 (s, 1H). ¹³C NMR (100 MHz, DMSO-d₆): δ 38.3, 44.9, 104.5, 118.0 (2C), 118.7, 119.6 (2C), 125.2 (2C), 125.6 (2C), 127.0, 127.1 (2C), 128.2, 128.9 (2C), 139.0, 143.3, 144.0, 157.9, 160.6, 173.0, 194.8.

4-((5-Oxo-7-phenyl-5,6,7,8-tetrahydroquinazolin-2-yl)amino)-N-(4-tolyl)benzenesulfonamide (8)

Compound **8** was obtained as a solid (91 mg, 20%) starting from compound **16b** (0.37 g) and 1-iodo-4-methylbenzene (0.25 g); m.p. 83–85 °C. ¹H NMR (400 MHz, DMSO-d₆): δ 2.10 (s, 3H), 2.67–2.73 (m, 2H), 2.97–3.04 (m, 2H), 3.54–3.56 (m, 1H), 7.26–7.30 (m, 2H), 7.34–7.40 (m, 3H), 7.82 (d, *J* = 9.2 Hz, 2H), 7.96–8.07 (m, 4H), 8.12 (d, *J* = 9.2 Hz, 2H), 8.91 (s, 1H), 10.82 (s, 1H), 11.21 (s, 1H). ¹³C NMR (100 MHz, DMSO-d₆): δ 20.9, 38.5, 41.7, 45.0, 118.1, 119.4 (2C), 123.1 (2C), 126.4 (2C), 127.2, 127.3 (2C), 129.0 (2C), 130.7 (2C), 132.0, 138.2, 139.8, 142.7, 143.5, 158.1, 161.0, 173.1, 195.1.

4-((7,7-Dimethyl-5-oxo-5,6,7,8-tetrahydroquinazolin-2-yl)amino)-N-phenylbenzenesulfonamide (9)

Compound **9** was obtained as a solid (0.12 g, 30%) starting from compound **16c** (0.32 g) and iodobenzene (0.23 ml); m.p. 215–217 °C. ¹H NMR (400 MHz, DMSO-d₆): δ 1.03 (s, 6H), 2.46 (s, 2H), 2.86 (s, 2H), 7.00 (t, *J* = 7.2 Hz, 1H), 7.09 (d, *J* = 8.8 Hz, 2H), 7.21–7.24 (m, 2H), 7.70 (d, *J* = 8.8 Hz, 2H), 7.95 (d, *J* = 8.8 Hz, 2H), 8.84 (s, 1H), 10.17 (s, 1H), 10.68 (s, 1H). ¹³C NMR (100 MHz, DMSO-d₆): δ 27.9, 32.4, 44.9, 51.2, 118.0, 119.2 (2C), 120.0, 124.0 (2C), 126.1, 127.9 (2C), 129.2 (2C), 129.8, 132.5, 143.5, 157.4, 160.7, 195.2.

4-((7,7-Dimethyl-5-oxo-5,6,7,8-tetrahydroquinazolin-2-yl)amino)-N-(4-methoxyphenyl)benzenesulfonamide (10)

Compound **10** was obtained as a solid (0.15 g, 35%) starting from compound **16c** (0.32 g) and 1-iodo-4-methoxybenzene (0.26 g); m.p. 210–212 °C. ¹H NMR (400 MHz, DMSO-d₆): δ 1.03 (s, 6H), 2.86 (s, 2H), 3.65 (s, 3H), 6.79 (d, *J* = 8.8 Hz, 2H), 6.98 (d, *J* = 8.8 Hz, 2H), 7.62 (d, *J* = 8.8 Hz, 2H), 7.93 (d, *J* = 8.8 Hz, 2H), 8.84 (s, 1H), 9.80 (s, 1H), 10.67 (s, 1H). ¹³C NMR (100 MHz, DMSO-d₆): δ 27.8, 32.4, 51.2, 55.2, 114.3 (2C), 119.1 (2C), 123.2 (2C), 127.8 (2C), 129.2, 130.5, 138.1, 143.2, 153.0, 153.8, 160.6, 166.4, 195.1.

4-((7,7-Dimethyl-5-oxo-5,6,7,8-tetrahydroquinazolin-2-yl)amino)-N-(4-nitrophenyl)benzenesulfonamide (11)

Compound **11** was obtained as a solid (0.13 g, 30%) starting from compound **16c** (0.32 g) and 1-iodo-4-nitrobenzene (0.28 g); m.p. 264–266 °C. ¹H NMR (400 MHz, DMSO-d₆): δ 1.04 (s, 6H), 2.87 (s, 2H), 7.32 (d, *J* = 8.8 Hz, 2H), 7.84 (d, *J* = 8.8 Hz, 2H), 8.02 (d, *J* = 9.2 Hz, 2H), 8.14 (d, *J* = 9.2 Hz, 2H), 8.85 (s, 1H), 10.74 (s, 1H), 11.19 (s, 1H). ¹³C NMR (100 MHz, DMSO-d₆): δ 27.7, 32.3, 44.8, 51.0, 117.7 (2C), 117.9, 119.3 (2C), 125.3 (2C), 127.9 (2C), 131.6, 142.3, 144.0, 144.4, 157.2, 160.5, 172.3, 195.0.

4-((7,7-Dimethyl-5-oxo-5,6,7,8-tetrahydroquinazolin-2-yl)amino)-N-(p-tolyl)benzenesulfonamide (12)

Compound **12** was obtained as a solid (0.10 g, 25%) starting from compound **16c** (0.32 g) and 1-iodo-4-methylbenzene (0.25 g); m.p. 246–248 °C. ¹H NMR (400 MHz, DMSO-d₆): δ 1.03 (s, 6H), 2.17 (s, 3H), 2.86 (s, 2H), 6.96–7.03 (m, 4H), 7.66 (d, *J* = 8.8 Hz, 2H), 7.93 (d, *J* = 8.8 Hz, 2H), 8.84 (s, 1H), 10.01 (s, 1H), 10.67 (s, 1H). ¹³C NMR (100 MHz, DMSO-d₆): δ 20.4, 27.9, 32.4, 45.9, 51.2, 119.0, 119.2 (2C), 120.4 (2C), 126.1, 127.8 (2C), 129.6 (2C), 130.3, 143.4, 143.8, 144.4, 157.2, 157.4, 195.1.

CA inhibition assays

An Applied Photophysics stopped-flow instrument was used for assaying the CA catalysed CO₂ hydration activity²⁸. Phenol red (at a concentration of 0.2 mM) was used as indicator, working at the absorbance maximum of 557 nm, with 10 mM Hepes (pH 7.5) as buffer, 0.1 M Na₂SO₄ (for maintaining constant ionic strength), following the CA-catalysed CO₂ hydration reaction for a period of 10–100 s. The CO₂ concentrations ranged from 1.7 to 17 mM for the determination of the kinetic parameters and inhibition constants. For each inhibitor at least six traces of the initial 5–10% of the reaction have been used for determining the initial velocity. The uncatalysed rates were determined in the same manner and subtracted from the total observed rates. Stock solutions of inhibitors (10 mM) were prepared in distilled-deionised water with 10% of DMSO and dilutions up to 0.01 μM were done thereafter with the assay buffer. The inhibitor and enzyme solutions were preincubated together for 15 min (standard assay at room temperature) prior to assay, to allow for the formation of the E-I complex. The inhibition constants were obtained by non-linear least-squares methods using PRISM 3 and the Cheng-Prusoff equation and represent the mean from at least three different determinations. Enzyme concentrations in the assay system were in the range of 5–12 nM.

Molecular modelling methods

Docking calculations were executed using the latest AutoDockGPU docking software²⁹ along with its GUI AutoDockTools (ADT)³⁰. The high-resolution X-ray crystal structure of hCA IX having (PDB 5FL4), hCA I (PDB 6EVR), hCA II (PDB 3K34), and hCA IV (PDB 5JN9)^{31–33} was downloaded and superimposed on the structure of hCA IX. Before docking, the co-crystal ligands of 5FL4, 6EVR, 3K34, and 5JN9 were removed. Later, the protein structures were prepared using the Protein Preparation Wizard of the Maestro suite^{34,35}. The Protein Preparation Wizard deletes water molecules, adds both bond orders and hydrogen atoms, and also produces the appropriate protonation states. Compound **3**, (*S*)-**5**, and (*R*)-**5** were constructed using the 2D sketcher tool of Maestro. The ligands were considered in all the possible flip conformations and appropriate protonation states were obtained. The ligand and protein files were then translated into the AD4 specific format (PDBQT) utilising the scripts `prepare_ligand4.py` and `prepare_receptor4.py`, respectively, with all the standard settings. Using AutoDock4_{Zn} forcefield protocol, the script `zinc_pseudo.py` was applied to add the tetrahedral pseudo atoms to the receptor PDBQT file³⁶. The grid boxes were centred on the active site of the protein. While creating the grid parameter files (GPF), the zinc-specific non-bonded pairwise potentials were also included. The dimensions of the grid boxes were defined with a set of grids of 60 Å×40 Å×50 Å along with the spacing of 0.375 Å. A total of 100 independent docking simulations were achieved for every possible conformation of compounds **3**, (*S*)-**5**, and (*R*)-**5**. Each docking calculation comprised 20 million energy evaluations utilising the Lamarckian genetic algorithm local search (GALS) method. All the dockings were performed with a population size of 250 and 300 runs of Solis and Wets local search with a probability of 0.6. A rate of mutation of 0.02 and a crossover rate of 0.8 were used to produce new docking attempts for following generations, and the best individual from each generation was propagated over the following generation. The docking modes of every 100 independent docking calculations of the ligand binding to the metalloenzyme were clustered based on a 2 Å cut-off value based on Cartesian coordinates of the atom and were also ranked based on free energy binding (ΔG_{AD4}). Compounds **3**, (*S*)-**5**, and (*R*)-**5** best conformations were selected based upon the predicted ΔG_{AD4} as well the cluster population.

Results and discussion

Chemistry

The key intermediates for the synthesis of all the new target compounds **1–12** were the bicyclic tetrahydroquinazoline derivatives **16a–c** already described by us¹⁵ belonging to class **V** (Chart 1). However, the synthetic procedure to obtain compounds **16a–c** has been here improved by exploiting MW irradiation as a valuable alternative to conventional heating, allowing to reach higher yields and shorter reaction times (40 min vs. 16 h). In detail, the commercially available 5-substituted-1,3-cyclohexanediones **13a–c** were reacted with an excess of *N,N*-dimethylformamide-dimethyl acetal (DMF-DMA) at 100 °C for 1 h, to furnish the intermediates **14a–c**. Then, MW-assisted condensation reaction between the proper bielectrophile 2-[(dimethylamino)methylene]cyclohexan-1,3-dione **14a–c**¹⁵ and the binucleophile guanidine **15**¹⁴ was performed to obtain crude compounds **16a–c** which were purified by recrystallisation from ethanol (Scheme 1).

The quinazolyl-*N*-arylbenzenesulfonamides **1–12** were then obtained by reacting compounds **16a–c** with the proper *p*-

substituted phenyliodide in acetonitrile (MeCN) in the presence of K₂CO₃, *N,N'*-dimethylethylenediamine (DMEDA), and CuI. The reaction mixture was heated at 100 °C and stirred for 8–24 h (TLC analysis); after cooling, the suspension obtained was filtered under reduced pressure and the solid was purified by flash chromatography, yielding the pure target derivatives **1–12**.

CA inhibition assays and structure–activity relationships

All the newly synthesised compounds **1–12** were investigated for their enzyme inhibitory ability against four physiologically relevant CA isoforms, namely the human hCA I, II, IV, and IX (Table 1), by a stopped-flow CO₂ hydrase assay using acetazolamide (AAZ, 5-acetamido-1,3,4-thiadiazole-2-sulphonamide, Chart 1) as the standard drug²⁸. Table 1 also reports the data referring to the parent primary sulphonamides **16a–c**¹⁵ for comparison purposes.

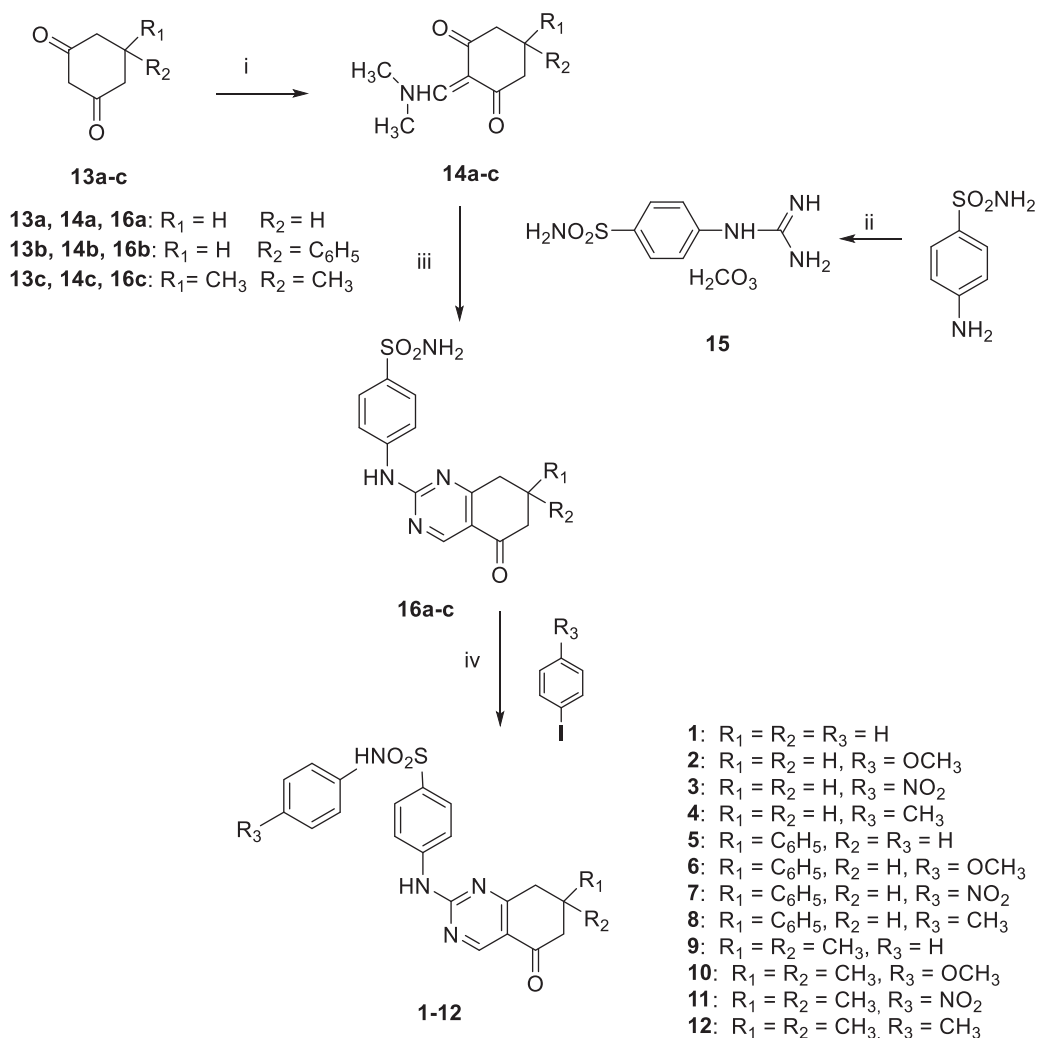
In particular, the inhibitory profile of the tetrahydroquinazolin-2-yl-amino-benzenesulfonamides **1–12** appears strictly dependent on the substitution pattern at 7-position, with few exceptions. Unsubstituted compounds (**1–4**) exhibit high potency against hCA IX (*K_i* values ranging from 0.42 μM to 1.04 μM), combined with an excellent selectivity with respect to the other isoforms tested. This trend appears to be independent of the decoration of the pendant phenyl ring (*R*₃).

The inhibitory potency of 7-phenyl derivatives (**5–8**) appears to be closely related to the decoration on the benzenesulfonamide moiety (*R*₃). hCA IX inhibition potency was maintained high when position 1 is unsubstituted (hCA IX, **5** *K_i* 0.45 vs. **1** *K_i* 0.42), and slightly decreased when *R*₃=OCH₃ or NO₂ (hCA IX, **6** *K_i* 1.73 and **7** *K_i* 1.33 vs. **2** *K_i* 0.46 and **3** *K_i* 0.42, respectively). The hCA IX-selectivity profile varied from excellent to good moving from *R*₃=H to *R*₃=NO₂ and *R*₃=OCH₃. Specifically, the best performing compound of the subseries in terms of hCA IX inhibitory potency and selectivity is the unsubstituted (*R*₃=H) compound **5**; the *p*-nitrophenyl-substituted analogue **7** (*R*₃=NO₂) results in a quite potent (*K_i* 1.33 μM) and selective (*K_i* ratio CAI/CAIX >75.2, CAII/CAIX 50.7, CAIV/CAIX >75.2) hCA IX inhibitor; the *p*-methoxy-substituted **6** (*R*₃=OCH₃), retains the hCA IX inhibitory potency of the same order of magnitude of **7** (*K_i* 1.73 μM), but the selectivity towards this isoform is considerably reduced (*K_i* ratio CAI/CAIX >19.6, CAII/CAIX 6.6, CAIV/CAIX >57.8). The presence of a methyl group at *R*₃ produced a marked reduction in hCA IX inhibitory potency (hCA IX: **8** *K_i* 15.7 vs. **4** *K_i* 1.04), and a loss of selectivity, being **8** equally potent on hCA II and hCA IX.

Insertion of a double methyl substitution at position 7 produced a dramatic drop in hCA IX inhibition potency and a general gain in activity towards the other hCAs tested, particularly for hCA II. The 7,7-dimethyl-quinazoliny-*N*-arylbenzenesulfonamides **9–12** inhibited all the CAs tested with micromolar potency (with few exceptions), showing a moderate selectivity for the hCA II isoform (*K_i* values from 5.1 to 22.4 μM). Only compound **12** (*R*₃=CH₃) did not register a gain in selectivity for the hCA II isoform showing comparable *K_i* values for all the tested hCA isoforms.

All in all, these data highlighted the identification of several hCA IX inhibitors with high potency and selectivity, featuring a secondary benzenesulfonamide on the tetrahydroquinazoline scaffold. The best-performing compounds are represented by **3** (*R*₁=*R*₂=H, *R*₃=NO₂) and **5** (*R*₁=H, *R*₂=C₆H₅, *R*₃=H), that are the most potent (**3** *K_i* 0.42 μM; **5** *K_i* 0.45 μM) and selective (*K_i* ratio CAI/CAIX, CAII/CAIX, CAIV/CAIX >238.1 and >222.2 for **3** and **5**, respectively) hCA IX inhibitors of this new series of derivatives.

It should be outlined that, comparing the most interesting new compounds **1–5** with the parent primary tetrahydroquinazolin-



Scheme 1. Reagents and conditions: (i) DMF-DMA, 100 °C, 1 h; (ii) conc HCl/50% cyanamide water solution, 100 °C, 0.5 h; (iii) *n*-butanol, NaOH, M.W. (40 min, 160 °C); (iv) MeCN, K₂CO₃, DMEDA, CuI, 100 °C, 8–24 h.

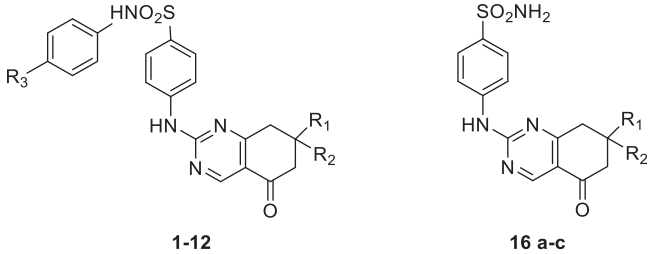
sulphonamides **16a–c**, despite the lower hCA IX inhibitory potency of the secondary **1–5**, their hCA IX selectivity is greater than that observed for primary sulphonamides **16a–c**. This greater selectivity is especially evident with respect to isoform II with *K_i* ratios CAII/CAIX ranging from 7.6 to 9.45 for **16a–c** and from 85.8 to >238 for **1–5**.

Furthermore, a comparison of the obtained results for **1–4** with those of the corresponding tetrahydroindazole-based secondary sulphonamides of series **VI** (**VIa–d** in Table 2) recently described by us¹⁶, highlighted that, by keeping the same R₃-substituents (R₃=H, *p*-OCH₃, *p*-NO₂, *p*-CH₃) and changing the scaffold from tetrahydroindazole (**VIa–d**) to tetrahydroquinazolinone (**1–4**), the good potency (*K_i* 1.4–5.7 μM) and selectivity towards the hCA I isoform shifted to high potency (*K_i* 0.42–1.04 μM) and excellent selectivity towards the hCA IX isoform. In particular, by comparing the *p*-nitro-substituted derivatives **3** and **VIc** (R₁=R₂=H, R₃=NO₂) which are the best performing compounds in the two subseries, a *K_i* value of 5.7 μM for **VIc** against hCA I with slight selectivity (*K_i* ratio CAII/CAI 8.8, CAIV/CAI 13.3, CAIX/CAI 14.7), and a *K_i* value of 0.42 μM against the hCA IX isoform with a high selectivity (*K_i* ratio CAI/CAIX, CAII/CAIX, CAIV/CAIX >238.1) for **3** are highlighted.

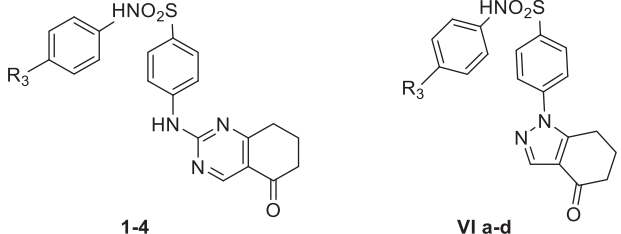
Molecular modelling studies

To rationalise the SAR data attained for various substitutions of newly designed secondary sulphonamides (Table 1), a series of molecular modelling studies were performed on compounds **3** and **5**, as they are the most potent inhibitors of hCA IX as well as the most selective over the other tested hCAs (I, II, and IV) of the whole set. In this process, the AutoDock4_{Zn} docking protocol, devised for docking experiments on zinc-chelating ligands, was employed as implemented in our previous reports on hCAs^{15,37}. The best docking solution, i.e. the one having the lowest predicted binding free energy, achieved for compound **3** in the hCA IX (PDB 5FL4)³¹ binding site is shown in Figure 1.

Mainly, the sulphonamide chelates the catalytic zinc ion through its negatively charged nitrogen atom in a geometry that is consistent with the other CAIs. Additionally, one of the sulphonamide oxygen atoms is well-positioned to accept an H-bond from the backbone NH of Thr201. Apart from these interactions, which were consistent with our previous reports on hCAs^{15,37}, it is also interesting to see that the phenyl ring, attached to the sulphonamide negative nitrogen, forms a π - π interaction with His98 and places its *p*-NO₂ group in a hydrophilic protein region at H-

Table 1. Inhibition of hCA isoforms I, II, IV, and IX with tetrahydroquinazoline derivatives 1–12, 16a–c, and AAZ as the reference standard by a stopped-flow CO₂ hydase assay.


Compound	R ₁	R ₂	R ₃	K _i (μM) ^a			
				hCA I [CA I/CA IX] ^b	hCA II [CA II/CA IX] ^b	hCA IV [CA IV/CA IX] ^b	hCA IX
1	H	H	H	89.1 [185.6]	41.2 [85.8]	>100 [>208]	0.48
2	H	H	OCH ₃	>100 [>217]	50.3 [109.3]	>100 [>217]	0.46
3	H	H	NO ₂	>100 [>238]	>100 [> 238]	>100 [>238]	0.42
4	H	H	CH ₃	>100 [>96]	>100 [> 96]	>100 [>96]	1.04
5	H	C ₆ H ₅	H	>100 [>222]	>100 [> 222]	>100 [>222]	0.45
6	H	C ₆ H ₅	OCH ₃	34.0 [19.6]	11.5 [6.6]	>100 [>57.8]	1.73
7	H	C ₆ H ₅	NO ₂	>100 [>75.2]	67.5 [50.7]	>100 [>75.2]	1.33
8	H	C ₆ H ₅	CH ₃	46.1	13.0	>100	15.7
9	CH ₃	CH ₃	H	70.5	7.4	91.1	47.3
10	CH ₃	CH ₃	OCH ₃	24.7	5.1	78.1	48.1
11	CH ₃	CH ₃	NO ₂	62.0	6.9	>100	>100
12	CH ₃	CH ₃	CH ₃	84.9	22.4	62.1	19.3
16a ^c	H	H	–	0.0639 [116]	0.0052 [9.45]	0.073 [132.7]	0.00055
16b ^c	H	C ₆ H ₅	–	>100 [869]	0.0060 [7.6]	0.078 [98.7]	0.00079
16c ^c	CH ₃	CH ₃	–	>100 [712]	0.0082 [9.2]	0.3194 [359]	0.00089
AAZ				0.25	0.012	0.074	0.026

^aMean from three different assays, by a stopped flow technique (errors were in the range of ±5–10% of the reported values).^bK_i ratio for the indicated enzyme isoforms.^cData from ref.¹⁵**Table 2.** Inhibition of hCA isoforms I, II, IV, and IX with tetrahydroquinazoline (1–4) tetrahydroindazole (VIa–d)¹⁶ and secondary sulphonamides.


Compound	R ₃	K _i (μM) ^a			
		hCA I	hCA II	hCA IV	hCA IX
1	H	89.1 [CA I/CA IX] ^b =185.6	41.2 [CA II/CA IX] ^b =85.8	>100 [CA IV/CA IX] ^b >208	0.48
2	OCH ₃	>100 [CA I/CA IX] ^b >217	50.3 [CA II/CA IX] ^b =109.3	>100 [CA IV/CA IX] ^b >217	0.46
3	NO ₂	>100 [CA I/CA IX] ^b >238	>100 [CA II/CA IX] ^b >238	>100 [CA IV/CA IX] ^b >238	0.42
4	CH ₃	>100 [CA I/CA IX] ^b >96	>100 [CA II/CA IX] ^b >96	>100 [CA IV/CA IX] ^b >96	1.04
VIa ^c	H	5.7	31.0 [CA II/CA I] ^b =5.4	59.6 [CA IV/CA I] ^b =10.4	97.9 [CA IX/CA I] ^b =17.2
VIb ^c	OCH ₃	1.4	5.9 [CA II/CA I] ^b =4.2	79.3 [CA IV/CA I] ^b =56.6	56.5 [CA IX/CA I] ^b =40.3
VIc ^c	NO ₂	5.7	50.3 [CA II/CA I] ^b =8.8	75.8 [CA IV/CA I] ^b =13.3	83.7 [CA IX/CA I] ^b =14.7
VId ^c	CH ₃	4.9	8.4 [CA II/CA I] ^b =1.71	52.5 [CA IV/CA I] ^b =10.7	39.2 [CA IX/CA I] ^b =8.0
AAZ		0.25	0.012	0.074	0.026

^aMean from three different assays, by a stopped flow technique (errors were in the range of ±5–10% of the reported values).^bK_i ratio for the indicated enzyme isoforms.^cData from ref.¹⁶

bonding distance to multiple residues such as Asn66, His68, and Gln71. These latter interactions might explain why compound **4**, featuring the lipophilic *p*-CH₃ group, by establishing less favourable interactions with the enzyme counterpart, is less active than compounds **1–3**. Interestingly, the same trend was recorded for the phenyl-substituted analogues **5–8**. The benzene ring of the benzenesulfonamide forms van der Waals interactions with Val121

and Leu199 while the attached pyrimidine ring of the tetrahydroquinazoline scaffold forms an H-bond with Gln92 residue. This latter interaction might explain why the tetrahydroquinazolines described in the present work are generally more potent than the previously reported tetrahydroindazoles¹⁶. Moreover, the oxygen atom enclosed in tetrahydroquinazoline is pointing towards the “selectivity hotspot” of the hCA IX binding site.

Dockings of both isomers of **5** allow postulating the absence of a stereoselective recognition by hCAIX as, in both cases, the predicted lowest energy conformation places the negatively charged sulphonamide nitrogen to chelate the Zn^{2+} (Figure 2) with an overall orientation resembling the one achieved for **3**.

In particular, the (*S*)-**5** docking suggests that the negative nitrogen connected to the secondary sulphonamide is chelating the zinc ion, while a sulphonamide oxygen is forming an H-bond with the backbone NH of Thr201. If compared to the binding pose achieved for **3**, the presence of the phenyl ring at position 7 of the tetrahydroquinazoline ring seems to induce a partial relocation of the ligand and inducing the loss of the H-bond interaction with Gln92, thereby explaining why compounds **5–8** are less active than their unsubstituted counterparts **1–4**. In (*S*)-**5**, this loss seems to be counterbalanced by the presence of several van der Waals contacts between the phenyl ring and Leu91, Gln92, and Val130 enzyme residues in the “selectivity hotspot”. (*R*)-**5** docking calculations indicate the presence of a similar interaction pattern (Figure 2(B)).

To explain the selectivity profiles of **3**, (*S*)-**5**, and (*R*)-**5**, docking calculations of these compounds were also attempted employing the published structures of hCA I (PDB 6EVR), hCA II (PDB 3K34), and hCA IV (PDB 5JN9)^{32,33}. Interestingly, analysis of the obtained results revealed a certain difficulty in predicting a binding pose featuring the chelation of the Zn^{2+} ion. To explain these theoretical results, the binding pose obtained for **3**, (*S*)-**5**, and (*R*)-**5** into the hCA IX structure and conducive of the Zn^{2+} chelation, was rigidly translated into the aligned binding sites of hCA I, hCA II, and hCA IV. From this analysis, it is clear that such a ligand orientation is unfeasible into the hCA I, hCA II as it would give rise to multiple steric clashes (Figures 3(A,B) and 4(A,B)). Concerning hCA

IV, no steric clashes were evidenced, while unfavourable electrostatic interactions between the hydrophilic “selectivity hotspot” of hCA IV and the ligands could be detected (Figures 3(C) and 4(D)). This should explain while compounds **3** and **5** are unable to efficiently inhibit hCA I, hCA II, and hCA IV.

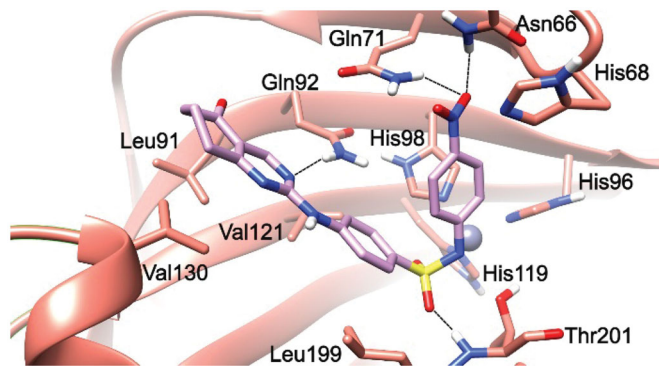


Figure 1. **3**/hCA IX theoretical complex (PDB 5FL4) computed by docking calculations. The protein is shaded in salmon and all the critical residues are labelled. The ligand is shown in pink colour while the H-bonds are shown in black dashed lines.

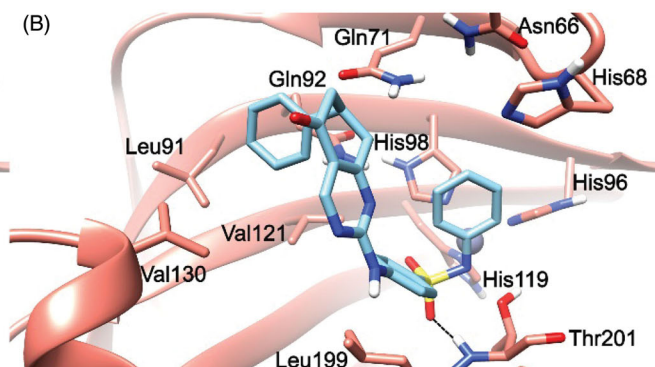
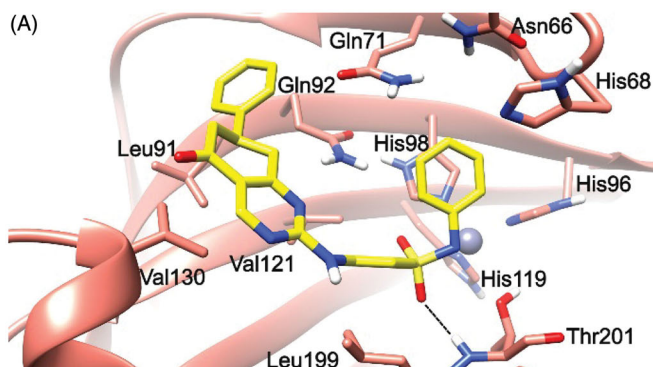


Figure 2. (*S*)-**5**/hCA IX (A) and (*R*)-**5**/hCA IX theoretical complexes (PDB 5FL4) computed by docking calculations. The protein is shaded in salmon and all the critical residues are labelled. The ligand is shown in yellow and cyan, respectively, while the H-bonds are shown in black dashed lines.

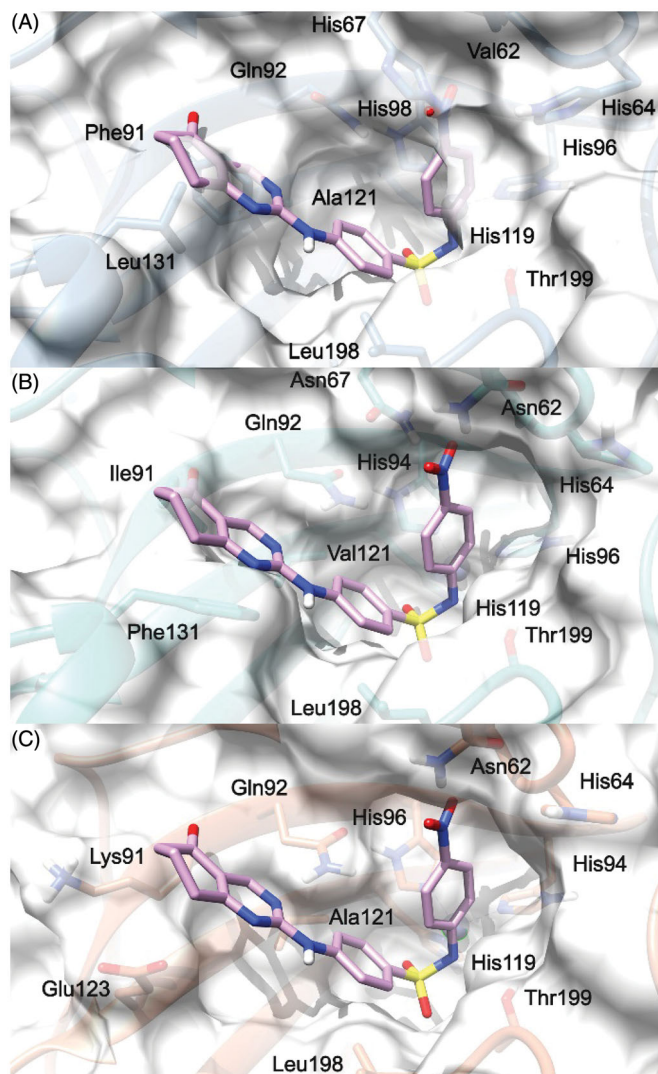


Figure 3. **3**/hCA IX theoretical binding pose translated into hCA I (PDB 6EVR, A), hCA II (PDB 3K34, B), and hCA IV (PDB 5JN9, C) structures. The proteins are shown in blue, sea-green, and coral ribbons and sticks, respectively, with their molecular surface shaded in white. The ligand is depicted in pink.

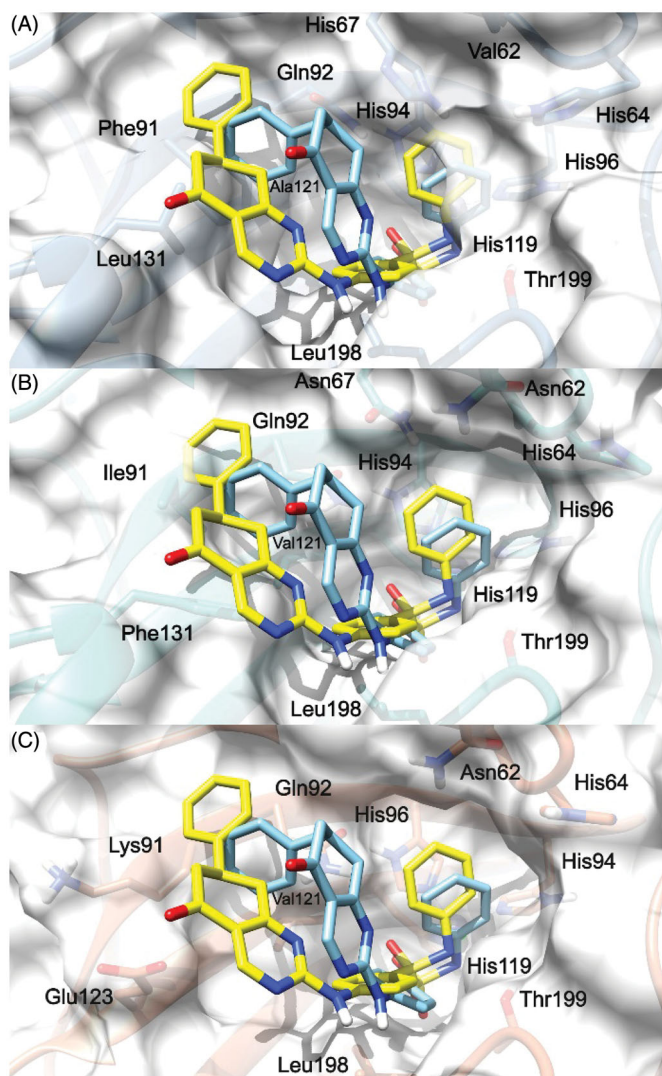


Figure 4. (S)-5 and (R)-5/hCA IX theoretical binding pose translated into hCA I (PDB 6EVR, A), hCA II (PDB 3K34, B), and hCA IV (PDB 5JN9, C) structures. The proteins are shown in blue, sea-green, and coral ribbons and sticks, respectively, with their molecular surface shaded in white. (S)-5 and (R)-5 are depicted in yellow and cyan sticks. All the pictures were rendered using UCSF chimera molecular visualisation software⁴⁰.

Conclusions

Within our project aimed at investigating the chemical space of secondary sulphonamide CAls, we herein reported the design, synthesis, and biological evaluation of a focussed library of variously decorated *N*-phenyl secondary sulphonamides featuring the bicyclic tetrahydroquinazole scaffold. Exploiting SAR studies from our previous work, we identified several compounds showing submicromolar potency and excellent selectivity for hCA IX, an isoform that has attracted significant interest as a putative cancer therapeutic target. SAR studies highlighted a strict correlation between the activity/selectivity profile and the substitution patterns at the 7-position of the central scaffold and the para-position of the benzenesulfonamide moiety of the target derivatives. Molecular modelling studies rationalised the SARs in terms of both inhibitory activity and selectivity profile. Overall, this study provided further information on the structural requirements for efficient and selective inhibition of the cancer-related hCA IX isoform and it could be useful for the design of novel anticancer agents. The class of secondary sulphonamides, although less investigated for their CA

inhibitory properties, may lead to relevant medicinal chemistry discoveries. Moreover, very recently Kennedy et al.³⁸ investigated inflammasome and pyroptotic pathways and identified a novel photoaffinity alkyne-tagged probe for such processes, compound belonging to the secondary sulphonamide class, which is also targeting efficiently CA II, confirming thus our earlier data^{16,25,39} that secondary sulphonamides effectively inhibit these enzymes, by a mechanism which starts to be elucidated through this and the above-mentioned works.

Disclosure statement

No potential conflict of interest was reported by the authors.

Funding

This work was supported by University of Campania Luigi Vanvitelli under Grant VALERE: Vanvitelli per la Ricerca, ANIMA and VALEREPlus projects, Campania and Regional Government Technology Platform Lotta alle Patologie Oncologiche under Grant iCURE, University of Pisa under Grant PRA_2020_58 and Italian MIUR under Grant PRIN 2017, 2017XYBP2R.

ORCID

Emma Baglini <http://orcid.org/0000-0002-8378-4052>
 Rahul Ravichandran <http://orcid.org/0000-0002-1908-6161>
 Emanuela Berrino <http://orcid.org/0000-0002-4258-0678>
 Silvia Salerno <http://orcid.org/0000-0002-6072-4698>
 Elisabetta Barresi <http://orcid.org/0000-0002-9814-7195>
 Anna Maria Marini <http://orcid.org/0000-0001-8664-375X>
 Monica Viviano <http://orcid.org/0000-0003-1118-790X>
 Federico Da Settimo <http://orcid.org/0000-0002-7897-7917>
 Claudiu T. Supuran <http://orcid.org/0000-0003-4262-0323>
 Sandro Cosconati <http://orcid.org/0000-0002-8900-0968>
 Sabrina Taliani <http://orcid.org/0000-0001-8675-939X>

References

- Supuran CT. Structure and function of carbonic anhydrases. *Biochem J* 2016;473:2023–32.
- Supuran CT. Carbonic anhydrases: novel therapeutic applications for inhibitors and activators. *Nat Rev Drug Discov* 2008;7:168–81.
- Supuran CT. Carbonic anhydrase inhibitors. *Bioorg Med Chem Lett* 2010;20:3467–74.
- Supuran CT. Carbonic anhydrase inhibitors and activators for novel therapeutic applications. *Future Med Chem* 2011;3: 1165–80.
- Supuran CT. Emerging role of carbonic anhydrase inhibitors. *Clin Sci* 2021;135:1233–49.
- Angeli A, Abdel-Aziz AAM, Nocentini A, et al. Synthesis and carbonic anhydrase inhibition of polycyclic imides incorporating *N*-benzenesulfonamide moieties. *Bioorg Med Chem* 2017;25:5373–9.
- Kurt BZ, Sonmez F, Ozturk D, et al. Synthesis of coumarin-sulfonamide derivatives and determination of their cytotoxicity, carbonic anhydrase inhibitory and molecular docking studies. *Eur J Med Chem* 2019;183:111702.
- Kurt BZ, Dag A, Doğan B, et al. Synthesis, biological activity and multiscale molecular modeling studies of bis-coumarins

- as selective carbonic anhydrase IX and XII inhibitors with effective cytotoxicity against hepatocellular carcinoma. *Bioorg Chem* 2019;87:838–50.
9. Awadallah FM, Bua S, Mahmoud WR, et al. Inhibition studies on a panel of human carbonic anhydrases with N1-substituted secondary sulfonamides incorporating thiazolinone or imidazole-indole tails. *J Enzyme Inhib Med Chem* 2018;33:629–38.
 10. Awadallah FM, El-Waei TA, Hanna MM, et al. Synthesis, carbonic anhydrase inhibition and cytotoxic activity of novel chromone-based sulfonamide derivatives. *Eur J Med Chem* 2015;96:425–35.
 11. Masini E, Carta F, Scozzafava A, Supuran CT. Antiglaucoma carbonic anhydrase inhibitors: a patent review. *Expert Opin Ther Pat* 2013;23:705–16.
 12. Alterio V, Di Fiore A, D'Ambrosio K, et al. Multiple binding modes of inhibitors to carbonic anhydrases: how to design specific drugs targeting 15 different isoforms? *Chem Rev* 2012;112:4421–68.
 13. Marini AM, Maresca A, Aggarwal M, et al. Tricyclic sulfonamides incorporating benzothiopyrano[4,3-c]pyrazole and pyridothiopyrano[4,3-c]pyrazole effectively inhibit α - and β -carbonic anhydrase: X-ray crystallography and solution investigations on 15 isoforms. *J Med Chem* 2012;55:9619–29.
 14. Barresi E, Salerno S, Marini AM, et al. Sulfonamides incorporating heteropolycyclic scaffolds show potent inhibitory action against carbonic anhydrase isoforms I, II, IX and XII. *Bioorg Med Chem* 2016;24:921–7.
 15. Salerno S, Barresi E, Amendola G, et al. 4-Substituted benzenesulfonamides incorporating bi/tricyclic moieties act as potent and isoform-selective carbonic anhydrase II/IX inhibitors. *J Med Chem* 2018;61:5765–70.
 16. Salerno S, Amendola G, Angeli A, et al. Inhibition studies on carbonic anhydrase isoforms I, II, IV and IX with N-arylsubstituted secondary sulfonamides featuring a bicyclic tetrahydroindazole scaffold. *Eur J Med Chem* 2021;220:113490.
 17. Wilkinson BL, Bornaghi LF, Houston TA, et al. A novel class of carbonic anhydrase inhibitors: glycoconjugate benzene sulfonamides prepared by “click-tailing”. *J Med Chem* 2006;49:6539–48.
 18. Güzel-Akdemir Ö, Akdemir A, Isik S, et al. O-Benzenedisulfonimido-sulfonamides are potent inhibitors of the tumor-associated carbonic anhydrase isoforms CA IX and CA XII. *Bioorg Med Chem* 2013;21:1386–91.
 19. Liu F, Martin-Mingot A, Lecornué F, et al. Carbonic anhydrases inhibitory effects of new benzenesulfonamides synthesized by using superacid chemistry. *J Enzyme Inhib Med Chem* 2012;27:886–91.
 20. Métayer B, Mingot A, Vullo D, et al. New superacid synthesized (fluorinated) tertiary benzenesulfonamides acting as selective HCA IX inhibitors: toward a new mode of carbonic anhydrase inhibition by sulfonamides. *Chem Commun* 2013;49:6015–7.
 21. Coviello V, Marchi B, Sartini S, et al. 1,2-Benzisothiazole derivatives bearing 4-, 5-, or 6-alkyl/arylcarboxamide moieties inhibit carbonic anhydrase isoform IX (CAIX) and cell proliferation under hypoxic conditions. *J Med Chem* 2016;59:6547–52.
 22. Ammazalorso A, Carradori S, Angeli A, et al. Fibrate-based N-acylsulphonamides targeting carbonic anhydrases: synthesis, biochemical evaluation, and docking studies. *J Enzyme Inhib Med Chem* 2019;34:1051–61.
 23. D'Ascenzio M, Guglielmi P, Carradori S, et al. Open saccharin-based secondary sulfonamides as potent and selective inhibitors of cancer-related carbonic anhydrase IX and XII isoforms. *J Enzyme Inhib Med Chem* 2017;32:51–9.
 24. Moeker J, Peat TS, Bornaghi LF, et al. Cyclic secondary sulfonamides: unusually good inhibitors of cancer-related carbonic anhydrase enzymes. *J Med Chem* 2014;57:3522–31.
 25. Alp C, Maresca A, Alp NA, et al. Secondary/tertiary benzene-sulfonamides with inhibitory action against the cytosolic human carbonic anhydrase isoforms I and II. *J Enzyme Inhib Med Chem* 2013;28:294–8.
 26. Supuran CT. How many carbonic anhydrase inhibition mechanisms exist? *J Enzyme Inhib Med Chem* 2016;31:345–60.
 27. Schenone P, Mosti L, Menozzi G. Reaction of 2-dimethylamino-methylene-1,3-diones with dinucleophiles. I. Synthesis of 1,5-disubstituted 4-acylpyrazoles. *J Heterocycl Chem* 1982;19:1355–61.
 28. Khalifah RG. The carbon dioxide hydration activity of carbonic anhydrase. I. Stop-flow kinetic studies on the native human isoenzymes B and C. *J Biol Chem* 1971;246:2561–73.
 29. Santos-Martins D, Solis-Vasquez L, Tillack AF, et al. Accelerating AutoDock4 with GPUs and gradient-based local search. *J Chem Theory Comput* 2021;17:1060–73.
 30. Morris G, Ruth H, Lindstrom W, et al. AutoDock4 and AutoDockTools4: automated docking with selective receptor flexibility. *J Comput Chem* 2009;30:2785–91.
 31. Leitans J, Kazaks A, Balode A, et al. Efficient expression and crystallization system of cancer-associated carbonic anhydrase isoform IX. *J Med Chem* 2015;58:9004–9.
 32. Chiamonte N, Bua S, Ferraroni M, et al. 2-Benzylpiperazine: a new scaffold for potent human carbonic anhydrase inhibitors. Synthesis, enzyme inhibition, enantioselectivity, computational and crystallographic studies and in vivo activity for a new class of intraocular pressure lowering agents. *Eur J Med Chem* 2018;151:363–75.
 33. Behnke CA, Le Trong I, Godden JW, et al. Atomic resolution studies of carbonic anhydrase II. *Acta Crystallogr D Biol Crystallogr* 2010;66:616–27.
 34. Schrödinger Release 2020-2: Protein Preparation Wizard; Epik, Schrödinger, LLC, New York, NY, 2020; Impact, Schrödinger, LLC, New York, NY; Prime, Schrödinger, LLC, New York, NY, 2020.
 35. Sastry GM, Adzhigirey M, Day T, Annabhimoju R, Sherman W. Protein and ligand preparation: Parameters, protocols, and influence on virtual screening enrichments. *J Comput Aid Mol Des* 2013; 27:221–34.
 36. Santos-Martins D, Forli S, Ramos MJ, Olson AJ. AutoDock4(Zn): an improved AutoDock force field for small-molecule docking to zinc metalloproteins. *J Chem Inf Model* 2014;54:2371–9.
 37. Milite C, Amendola G, Nocentini A, et al. Novel 2-substituted-benzimidazole-6-sulfonamides as carbonic anhydrase inhibitors: synthesis, biological evaluation against isoforms I, II, IX and XII and molecular docking studies. *J Enzyme Inhib Med Chem* 2019;34:1697–710.
 38. Kennedy CR, Goya Grocin A, Kovačić T, et al. A probe for NLRP3 inflammasome inhibitor MCC950 identifies carbonic anhydrase 2 as a novel target. *ACS Chem Biol* 2021;16:982–990.
 39. Nocentini A, Angeli A, Carta F, et al. Reconsidering anion inhibitors in the general context of drug design studies of modulators of activity of the classical enzyme carbonic anhydrase. *J Enzyme Inhib Med Chem* 2021;36:561–80.
 40. Pettersen EF, Goddard TD, Huang CC, et al. UCSF Chimera—a visualization system for exploratory research and analysis. *J Comput Chem* 2004;25:1605–12.